

Experimental determination of the enthalpy of mixing of N + CO₂ under pressure

ARUN V. HEJMADI, DONALD L. KATZ, and JOHN E. POWERS

*Department of Chemical and Metallurgical Engineering,
The University of Michigan, Ann Arbor, Michigan 48104, U.S.A.*

(Received 24 July 1970; in revised form 4 February 1971)

A once-through flow-calorimetric facility for measuring the enthalpy of mixing of binary gas mixtures at elevated pressures is described. The design of a new flow calorimetric incorporated in the facility is presented. Results for N₂+CO₂ from mole fraction of nitrogen 0.22 to 0.73 are reported at the nominal conditions 40 °C: 34.02 and 64.64 atm, and 31 °C: 34.02 and 64.64 atm. The experimental results are interpreted and smoothed, and compared with predictions using the Benedict-Webb-Rubin equation of state. The probable accuracy of the results is discussed, along with a check on the assumption of adiabaticity in the calorimeter.

1. Introduction

Precise enthalpies of pure compounds and mixtures are essential for purposes of evaluating theoretical calculations needed for engineering design. Enthalpies of mixing (or excess enthalpies) are particularly important since they link directly the enthalpy of a mixture to the enthalpies of its pure components. The molar enthalpy H_{A+B} of a mixture of A+B can be obtained by combining the molar excess enthalpy H^E with the molar enthalpies H_A and H_B of its pure components:

$$H_{A+B} = x_A H_A + x_B H_B + H^E, \quad (1)$$

where x denotes mole fraction.

Many calorimetric determinations of the enthalpy of mixing of liquids have been made, but very few gas mixtures have been so investigated. Pioneering work was done at the Kamerlingh Onnes laboratory⁽¹⁻⁴⁾ where the enthalpy of mixing of binary mixtures of H₂, He, N₂, Ar, and CH₄ were measured in a flow calorimeter. Klein⁽⁵⁾ made similar measurements on N₂+CH₄. The only available excess enthalpies of N₂+CO₂ are the published results of Lee and Mather.⁽⁶⁾ They also report excess enthalpies of N₂+H₂. Jacobsen and Baricau⁽⁷⁾ have investigated He+N₂. These are the only direct calorimetric measurements of the enthalpy of mixing of gases under pressure known to the authors.

This contribution describes the design of a new calorimetric facility and presents results for the enthalpy of mixing of N₂+CO₂. Considerable effort was expended to obtain accurate results as will be revealed in a discussion of the precision of the individual measurements.

the flow meters, 5 and 6.† Following the metering, the gases are expanded through manually operated valves, 21 and 22, to the conditioning coils (15 m in length) in the calorimeter bath on the way to the calorimeter. A low pressure (5 atm) flow meter, 19, is installed for metering the mixture but is used only for operational control. Under conditions of normal operation, the mixture is vented to the atmosphere. The two way solenoid valve, 23, is used only during flowmeter calibration to divert the flow of gas temporarily into the calibration tank.

CALORIMETER

The calorimeter is shown in figure 2. The primary feature of the calorimeter is to mix gases and add heat so that the mixture is returned to the inlet temperature before it is exposed to the surroundings. The two gases are mixed at 7 and then passed over an electrical resistance coil on the innermost of a series of concentric cylindrical shells which provide both mixing and a heat shield. The gas leaving the outermost shell passes through a helical tube, 9, wound around the capsule, conveying the gas to the thermocouple well, 11a. An added (gold plated) heat shield, 22, surrounds the helical coil to reduce radiant heat transfer. All of the above described are within a jacketed and evacuated space (1 to 5 m Torr pressure). A thin silver-plated copper radiation shield (dotted line), 23, stands between the mixing assembly and the outer vacuum jacket.

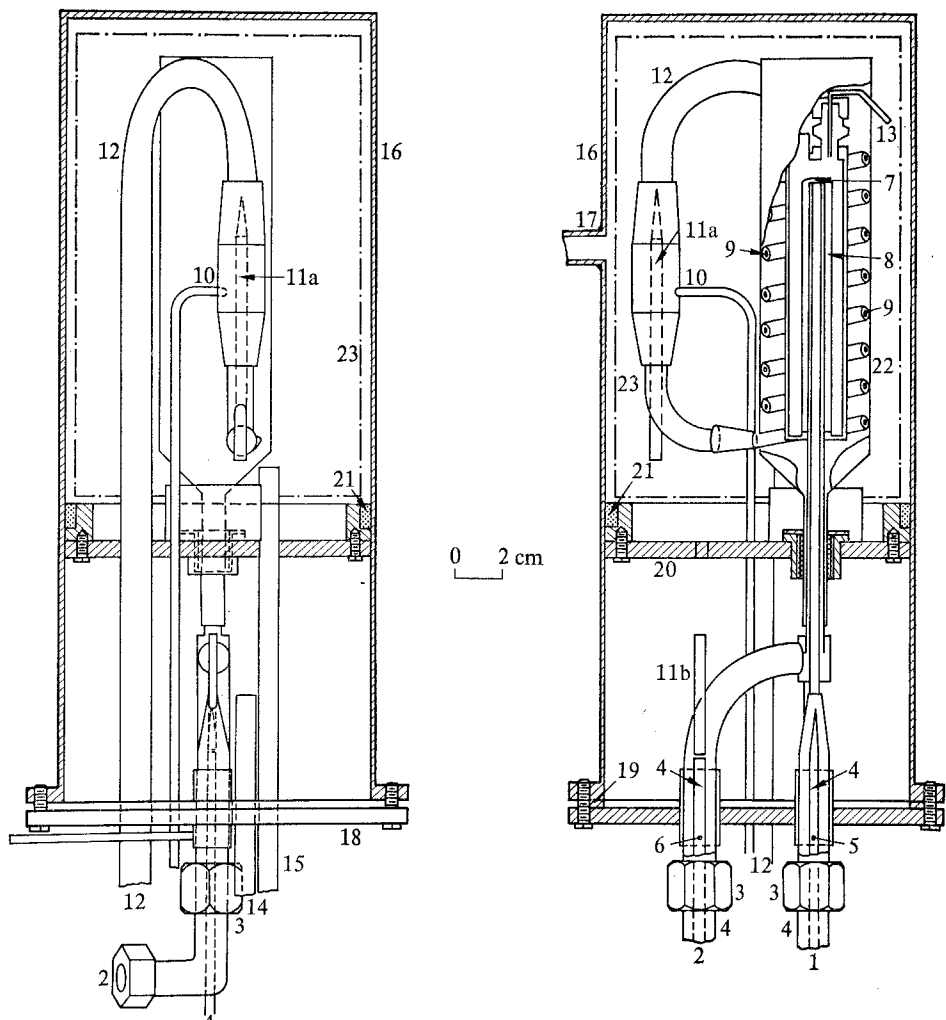
MEASUREMENTS AND CALIBRATIONS

The prime measurements are pressure, temperature, flow rate, gas composition, and electrical power input.

The temperature of the calorimeter bath is measured with an NBS-calibrated mercury-in-glass thermometer (range -1 to 51 °C and 0.1 °C smallest division on the International Practical Temperature Scale) with an uncertainty of ± 0.03 °C. The temperature of the entering nitrogen stream is assumed to be equal to the bath temperature. The temperature differences are measured between the two inlet streams (wells 4) by duplicate pairs of 6-junction copper-to-constantan thermopiles (these did not exceed 0.002 °C) and likewise with similar duplicate thermopiles between the inlet, 11b, and the outlet, 11a, thermowells. One of the latter thermopiles was calibrated by the NBS. A Leeds and Northrup Null Potentiometer was used to measure the output of the thermopiles. The accuracy of the temperature difference is estimated to be ± 0.006 °C based on the accuracy of the potentiometer, thermopile calibration, and the calorimeter bath control.

Pressures are measured within ± 0.02 atm at the calorimeter outlet tap, 10, by using a Mansfield & Green Model 13Q dead weight pressure balance with a certificate traceable to NBS. The technique suggested by Cross⁽⁸⁾ is employed in reducing dead-weight gauge readings to pressures. Atmospheric pressure is read to ± 0.5 Torr on a Fortin-type Eberbach barometer which has been calibrated against a standard barometer. Details of these measurements will be presented elsewhere.⁽⁹⁾ The pressure differences between pairs of taps 5, 6, 10 in the calorimeter are measured to establish both the uniformity of the entrance pressures and the pressure drop across the calori-

† Throughout this paper atm = $101\,325\text{ N m}^{-2}$ and Torr = atm/760.



- 1, Gas inlet A.
- 2, Gas inlet B.
- 3, 1 cm tubing union tees.
- 4, Thermocouple wells to measure differential temperature at inlet.
- 5, Inlet pressure tap—gas A.
- 6, Inlet pressure tap—gas B.
- 7, Mixing point of gases A and B.
- 8, Concentric mixing shells.
- 9, Helical tubes carrying mixed gases to outlet tubes.
- 10, Output pressure tap—mixture A + B.
- 11a, Outlet thermocouple well.
- 11b, Inlet thermocouple well to measure temperature differential between gas inlet and gas outlet. (Thermocouple junctions placed in wells 11a and 11b.)

- 12, Gas outlet tube.
- 13, Heater leads.
- 14, Tube for housing thermocouple lead.
- 15, Tube for housing heater leads.
- 16, Outer vacuum jacket.
- 17, Vacuum line.
- 18, Bottom flange.
- 19, Teflon gasket.
- 20, Teflon mechanical partition.
- 21, Brass collar with coarse interrupted threads; collar attached to outer jacket.
- 22, Gold-plated thin copper shield.
- 23, Silver-plated thin copper shield.

The sketch on the right shows details of the inlet assembly and mixing chamber.

FIGURE 2. Enthalpy of mixing calorimeter.

meter. The pressure drop is read in a Meriam high pressure manometer with dibutyl phthalate manometric fluid (density approximately 1.04 g cm⁻³). The thermal expansion characteristics are given by the Meriam Instrument Company who supplied the fluid. The pressure drops in one of the flow meters and in the calorimeter are measured with the same manometer. During an enthalpy of mixing measurement the pressure drop in the flow meters is monitored continuously with the manometer and telescope-cathetometer arrangement. However, the pressure drop in the calorimeter is read immediately after taking an experimental enthalpy of mixing reading with the same manometer. Hence, though the accuracy of the pressure drop measurement in the flow meter is ± 0.4 Torr, for the calorimeter the accuracy of this measurement is believed to be just ± 10 Torr.

Power is supplied to the calorimeter by a Kepco CK40-0.8M d.c. power supply with regulation to ± 0.01 per cent, and is determined by measuring potential drops across NBS calibrated standard resistors with the K-3 potentiometer. The Leeds and Northrup 7309 standard cell used in these measurements is checked at frequent intervals against a standard cell calibrated by NBS. Precautions were taken so that the limit of accuracy of the power input measurement was 0.1 per cent. Details of the wiring diagram will be given elsewhere.⁽⁹⁾

Metering of the flow rate is the most critical of all the measurements since the accuracy of the flow measurement is the limiting factor in the entire set of measurements. Only the salient features are given here. Details will be presented elsewhere.⁽⁹⁾ Each of the high pressure flow meters consists of a 33 cm length of 0.32 cm o.d. by 0.1 cm i.d. stainless steel tubing that is held rigid, sandwiched between two plates. The pressure drop determinations are made between pressure taps spaced 8.9 cm from each end. The flow meters are operated at a nominal pressure of 75 atm.

The pressure drops in the two flowmeters are registered in two separate Meriam high pressure manometers (dibutyl phthalate manometric fluid). The temperature of the fluid in the manometers is measured with a thermometer taped to the manometer well. The maximum measurable pressure drop is 1000 Torr and it is read to ± 0.4 Torr with a telescope cathetometer arrangement. The pressure at the flowmeter inlet pressure tap is measured with a Heise Bourdon tube gauge which is frequently calibrated against a dead weight pressure balance. The flowmeters are in a constant temperature bath held at (45 ± 0.01) °C.

Calibration is accomplished by flowing for a measured period of time under steady state conditions into a tank (calibration tank) of accurately determined volume, (0.1819 ± 0.0004) m³. Details of the tank volume determination and of the flow meter calibration procedure will be given elsewhere.⁽⁹⁾

The flowmeter calibration results are fitted to a modified version of the universal friction factor law.⁽¹⁰⁾ Viscosities η and densities ρ of the gas at the conditions in the flowmeter along with flowrate F are substituted in the equation:

$$F/\rho\Delta p = \alpha \log (\rho\Delta p/\eta^2) + \beta. \quad (2)$$

The accuracy of the flow metering of each gas is estimated to be 0.48 to 0.57 per cent based on the precision of the measuring instruments and the accuracy of the calibration tank volume determination.⁽⁹⁾

The gas composition of the stream leaving the calorimeter is measured by a modified gas density technique of which details will be given elsewhere.⁽¹³⁾ The uncertainty of the mole fraction determined with this technique is believed to be better than 0.006. The uncertainty in the mole fraction as calculated from a knowledge of the pure gas flow rates is estimated to be ± 0.002 to 0.003. Table 1 lists the mole fractions for a few cases determined by the two independent methods. The agreement is within the combined uncertainty of the two methods. This analytical technique provides a valuable check on the crucial measurements of the flow rates of the pure gases. Further, since a sample is taken and analyzed for every composition, temperature,

TABLE 1. Comparison of mole fractions x calculated from flowmeter calibrations with compositions measured using gas density technique for $N_2 + CO_2$.

$t_n/^\circ C$	p_n/atm	$x(N_2)$		$\Delta x(N_2)$
		Flowmeter calibrations	Gas density analysis	
40	34.02	0.503	0.506	+0.003
40	34.02	0.670	0.669	-0.001
40	64.64	0.358	0.360	+0.002
31	34.02	0.363	0.363	+0.000
31	64.64	0.239	0.242	+0.003

and pressure in the calorimeter corresponding to a measurement, the flow-meter calibrations are automatically checked for drifts and changes.

The impurities in the gases used are 0.09 mole per cent O_2 and 0.05 mole per cent N_2 in the CO_2 , and 0.02 mole per cent O_2 in the N_2 .

OPERATION

Before starting a run, the calorimeter and flow meter baths are set at predetermined temperatures and the valves on the gas supply cylinders are opened. The pressure in the flow meters is set initially at 75 atm by regulators, 3, (figure 1). The flow rates of the two pure gases are established by adjusting the metering valves, 21, thereby setting the mole fraction of the gas mixture in the calorimeter within 0.01 to 0.02 of a preselected value. Simultaneously the pressure in the calorimeter is brought to within ± 0.07 atm of the desired value by adjusting pressure reducing valve, 18. The power input to the calorimeter is then varied until the temperature of the outlet gas mixture is within $0.05^\circ C$ of the inlet pure gas temperature. Steady conditions are achieved 1 to 2 h after commencing gas flows. The calorimeter itself can attain a steady state within 15 to 20 min after a change in the input power setting if the initial values of the outlet and inlet gas temperatures differ by no more than $0.5^\circ C$. When all instrument readings indicate steady state conditions, readings are taken every 2 min and averaged over a 4 to 6 min period. Simultaneously, the mixture leaving the calorimeter is sampled for analysis. At the conclusion of the temperature measurements, the pressure differential measurements are made.

3. Results

Results are reported at the following nominal conditions in each case for at least four compositions: $t_n = 40^\circ\text{C}$, $p_n = 34.02\text{ atm}$ and $p_n = 64.64\text{ atm}$; and $t_n = 31^\circ\text{C}$, $p_n = 34.02\text{ atm}$ and $p_n = 64.64\text{ atm}$. The first four columns of table 2 give the raw results from the calorimetric and flow measurements for the outlet temperature t_0 and pressure p_0 , mole fraction $x(\text{N}_2)$ of N₂, and ratio P/F of power input P to molar flow rate F .

4. Analysis of results

The flow calorimeter has two reasonably pure streams entering it: one of A at temperature t_1 and pressure p_1 and one of B at t_2, p_2 ; and one stream of a mixture of A + B leaving it at t_0, p_0 . The first law of thermodynamics, when applied to this system at a

 TABLE 2. Enthalpies of mixing of N₂+CO₂

t_0 °C	p_0 atm	$x(\text{N}_2)$	$\frac{P}{F}$ J mol ⁻¹	$\frac{H_0^E}{J\text{ mol}^{-1}}$	$\frac{H_n^E}{J\text{ mol}^{-1}}$	$10^2 \frac{H_{\text{expt}}^E - H_{\text{calc}}^E}{H_{\text{expt}}^E}$
Nominal experimental conditions: $t_n = 40^\circ\text{C}$; $p_n = 34.02\text{ atm}$						
40.037	34.23	0.288	178.7	179.3	178.3	0.47
40.064	34.02	0.339	187.2	187.5	187.5	-0.49
40.049	34.00	0.437	196.7	195.7	195.9	-0.33
40.068	34.03	0.481	194.8	194.8	194.8	-0.38
40.001	33.89	0.482	195.3	194.2	195.1	-0.16
40.011	34.12	0.484	195.5	196.2	195.6	0.11
40.037	34.07	0.491	195.3	195.3	195.0	0.08
40.014	33.99	0.503	192.9	193.2	193.5	-0.21
40.036	34.03	0.508	196.1	194.4	194.5	0.47
40.015	33.86	0.509	193.7	193.1	194.3	0.45
40.013	33.81	0.510	193.8	192.7	194.2	0.44
40.033	33.92	0.518	191.5	191.6	192.4	-0.09
40.017	33.97	0.525	191.8	192.0	192.4	0.31
40.033	34.03	0.575	186.0	185.4	185.5	0.56
40.001	34.02	0.670	161.9	161.6	161.6	-0.35
Nominal experimental conditions: $t_n = 40^\circ\text{C}$; $p_n = 64.64\text{ atm}$						
40.088	64.62	0.220	626.4	624.4	627.2	0.76
39.955	64.81	0.358	705.1	711.6	705.5	-0.64
40.105	64.38	0.516	656.0	653.8	662.7	0.94
39.991	64.36	0.732	437.0	439.6	444.0	-0.14
Nominal experimental conditions: $t_n = 31^\circ\text{C}$; $p_n = 34.02\text{ atm}$						
31.023	34.02	0.228	180.5	180.3	180.3	-0.02
31.009	34.18	0.363	222.7	223.1	221.3	0.35
30.994	34.22	0.485	226.0	226.7	224.6	-0.29
30.990	33.90	0.729	163.5	164.1	165.0	0.02
Nominal experimental conditions: $t_n = 31^\circ\text{C}$; $p_n = 64.64\text{ atm}$						
31.064	64.45	0.239	976.6	975.5	991.4	1.17
31.003	64.61	0.310	1024.4	1029.9	1032.0	-0.76
31.047	64.55	0.489	953.3	955.0	961.7	0.93
31.010	64.82	0.725	602.9	605.0	600.0	-0.06

steady state with negligible potential energy effects reduces to

$$(P + \dot{q})/F = H_{A+B,0} - x_A H_{A,1} - x_B H_{B,2} + E_{k,A+B,0} - x_A E_{k,A,1} - x_B E_{k,B,2} \quad (3)$$

where P denotes power input to the calorimeter, \dot{q} rate of heat leak into the calorimeter, F molar flow rate, x mole fraction, H molar enthalpy, and E_k molar kinetic energy.

The excess enthalpy H^E as defined by equation (1) cannot be calculated directly from this equation because there are minor but measurable differences between inlet and outlet temperatures and pressures. It is convenient to determine H_0^E at the outlet conditions t_0 and p_0 in the calorimeter. Combining equations (1) and (3), and assuming zero heat leak, $\dot{q} = 0$, yields

$$H_0^E = P/F + x_A(H_{A,1} - H_{A,0}) + x_B(H_{B,2} - H_{B,0}) + \Delta E_k, \quad (4)$$

where

$$\Delta E_k = x_A E_{k,A,1} + x_B E_{k,B,2} - E_{k,A+B,0}. \quad (5)$$

The quantities in parentheses in equation (4) are given by

$$H_{A,1} - H_{A,0} = \int_{p_0}^{p_1} \phi_A dp + \int_{t_0}^{t_1} C_{p,A} dt, \quad (6a)$$

$$H_{B,2} - H_{B,0} = \int_{p_0}^{p_2} \phi_B dp + \int_{t_0}^{t_2} C_{p,B} dt, \quad (6b)$$

where

$$\phi = (\partial H / \partial p)_T, \quad (6c)$$

$$C_p = (\partial H / \partial T)_p. \quad (6d)$$

The two quantities ϕ and C_p are related to the Joule-Thomson coefficient μ by

$$\mu = -\phi / C_p. \quad (7)$$

Thus a set of primary corrections defined by equations (5) and (6) have to be applied to P/F according to equation (4) to obtain H_0^E at the conditions at the outlet of the calorimeter, t_0 and p_0 . The correction for kinetic energy differences is defined by (5) and requires the densities of the two pure components and of the mixtures. The corrections for pressure drops and temperature differences in (6) require thermodynamic data on the pure components only. Corrections are also made for the impurities in the inlet gas streams.

A set of secondary adjustments (hereafter called secondary corrections) is applied to H_0^E calculated from equation (4) to obtain H_n^E . The data are normalized to a common temperature t_n and pressure p_n in order to compensate for the small operational variations in outlet conditions, t_0 and p_0 . Thermodynamic data on the mixture are required:

$$H_n^E = H_0^E + \int_{p_0}^{p_n} \phi^E dp + \int_{t_0}^{t_n} C_p^E dt, \quad (8a)$$

where

$$\phi^E = (\partial H^E / \partial p)_{T,x}, \quad (8b)$$

$$C_p^E = (\partial H^E / \partial T)_{p,x}. \quad (8c)$$

PRIMARY CORRECTIONS

Kinetic energy corrections are calculated using densities from tabulations on N₂ by Din⁽¹¹⁾ and on CO₂ by Newitt *et al.*,⁽¹²⁾ and compressibility factors for N₂+CO₂ from Haney and Bliss.⁽¹³⁾ Table 3 shows a typical correction due to the term ΔE_k , the maximum contribution of which is 10⁻⁴ per cent.

Corrections for pressure drop and for non-isothermal operation are made employing C_p tabulations for N₂ by Din⁽¹¹⁾ and for CO₂ by Vukalovich and Altunin,⁽¹⁴⁾ and Joule-Thomson coefficients of pure CO₂ and N₂ from Roebuck *et al.*^(15,16) The pressure drop correction is the smaller of the two and it decreases with increased density of the gases flowing through the calorimeter as can be seen in the two examples in table 3. The average contribution of this correction is 0.1 per cent with a maximum

 TABLE 3. Examples of corrections used to obtain H_0^E and H_n^E from P/F for N₂+CO₂

Nominal experimental conditions	$t_n/^\circ\text{C}$	40	31
	p_n/atm	34.02	64.64
Actual experimental conditions (conditions at outlet of calorimeter)	$t_o/^\circ\text{C}$	40.033	31.010
	p_o/atm	33.92	64.82
$x(\text{N}_2)$		0.518	0.725
$(P/F)/\text{J mol}^{-1}$		191.5	602.9
Primary corrections: applied to P/F		Per cent corrections	
(a) For pressure drop across calorimeter		-0.22	-0.03
(b) For non-isothermal operation		-0.07	-0.10
(c) For kinetic energy difference of incoming and outgoing gases		-8×10^{-4}	0.5×10^{-5}
(d) For impurities in CO ₂		0.37	0.48
	Total:	0.08	0.35
$H/\text{J mol}^{-1}$		191.6	605.0
Secondary corrections: applied to H_n^E			
(e) For normalizing to p_n		0.34	-0.86
(f) For normalizing to t_n		0.03	0.04
	Total:	0.37	-0.82
$H^E/\text{J mol}^{-1}$		192.4	600.0

of 0.22 per cent. The correction for the temperature discrepancy between the inlet and outlet gases to the calorimeter averages about 0.5 per cent with a maximum of 1.2 per cent.

The effect of impurities in the two inlet gas streams is taken into account by assuming that oxygen and nitrogen have negligible enthalpy of mixing. Corrections are then calculated by assuming that the nitrogen stream contains no impurities and the carbon dioxide stream contains 0.14 mole per cent of nitrogen. The experimental results of this research are used to make the corrections for the nitrogen in the inlet carbon dioxide stream. The derivation of the equations used to make these corrections will be presented elsewhere.⁽⁹⁾ This correction ranges between 0.3 and 0.8 per

cent with an average contribution of 0.5 per cent. These four corrections are illustrated in table 3. The primary corrections do not affect the precision of the calorimetric measurements appreciably as the data in the literature are reliable and the corrections are small. The values of H_0^E calculated by applying the primary corrections to the values of P/F given in column 4 of table 1 are given in column 5 of table 2.

SECONDARY CORRECTIONS

These are applied to the excess enthalpies H_0^E at the outlet conditions of the calorimeter, and are also illustrated in table 3.

Uncertainties in the corrections for pressure and temperature level exceed the uncertainties in the previous corrections because there are no direct experimental data available on ϕ^E and C_p^E defined by equation (8) for $N_2 + CO_2$. These differentials are calculated using the original Benedict-Webb-Rubin⁽¹⁷⁾ equation of state with Bloomer and Rao's⁽¹⁸⁾ constants for N_2 , and Cullen and Kobe's⁽¹⁹⁾ constants for CO_2 with mixing rules suggested by Benedict *et al.*⁽²⁰⁾ Values of ϕ^E calculated from the B. W. R. equation of state at 40 °C agree within 10 per cent at 35 atm and within 30 per cent at 65 atm with values obtained by differentiating Lee and Mather's⁽⁶⁾ data. The normalized values of H_n^E calculated by applying the secondary corrections to the values of H_0^E in column 5 of table 2 are shown in column 6 of table 2.

5. Smoothing of results

Primary and secondary corrections having been applied, the excess enthalpies are smoothed by a least squares analysis. Smoothed results obtained at several flow rates are used to make a check on the assumption of adiabaticity.

Regular solution theory predicts:

$$H^E/x(1-x) = \text{constant.} \quad (9)$$

Therefore the equation used in correlating the results is

$$H^E/x(1-x) = A + B(x-0.5) + C(x-0.5)^2, \quad (10)$$

where x is used to denote the mole fraction $x(N_2)$ of nitrogen.

Coefficients for this equation are listed in table 4 with an average percentage deviation of the experimental points from this curve. The last column in table 2 lists

TABLE 4. Regression coefficients for the equation:
 $H^E/x(1-x) = A + B(x-0.5) + C(x-0.5)^2$
 where x denotes the mole fraction of N_2 in $N_2 + CO_2$

Experimental conditions		Regression coefficients			Percentage arithmetical average absolute deviation from experimental points	100 σ
t °C	p atm	A J mol ⁻¹	B J mol ⁻¹	C J mol ⁻¹		
40	34.02	777.310	-326.125	422.907	0.32	0.40
40	64.64	2670.80	-2519.96	3393.29	0.57	1.29
31	34.02	896.086	-362.753	430.894	0.19	0.45
31	64.64	3766.21	-4711.35	6108.36	0.70	1.72

the deviation of every experimental point as $100(H_{\text{expt}}^E - H_{\text{calc.}}^E)/H_{\text{expt}}^E$. The smoothed values calculated from equation (10) are plotted as solid lines in figures 3, 4, and 5. The circles in these figures are experimental values of H_n^E after primary and secondary corrections have been applied.

There are considerable deviations, due perhaps to the proximity of the critical of CO_2 , from regular solution theory. Thus the peak in figure 3 is skewed toward high mole fractions of CO_2 and the curves in figures 4 and 5 slant sharply instead of being horizontal as predicted by regular solution theory.

CHECK ON THE ASSUMPTION OF ADIABATICITY

This is essential since the application of equation (4) assumes zero heat leaks from the calorimeter. Based on a principle suggested by Montgomery and DeVries,⁽²¹⁾ excess enthalpies are measured over a range of flow rates to determine whether they are independent of flow rate. The ten points in figure 6 represent experimental results normalized to mole fraction 0.5 of N_2 , 34.02 atm, and 40 °C. The compositions all lie between mole fractions 0.48 and 0.524 of N_2 and are listed in table 2. These same data are the cluster of points at about mole fraction 0.50 in both figures 3 and 4 at 34.02 atm and 40 °C.

The standard deviation of the ten points from the average value of 194.2 J mol^{-1} is 0.31 per cent. A straight line was fitted to these ten points in figure 6 by a regression analysis. The intercept of this line at infinite flow rate ($f^{-1} \rightarrow 0$) deviated from the

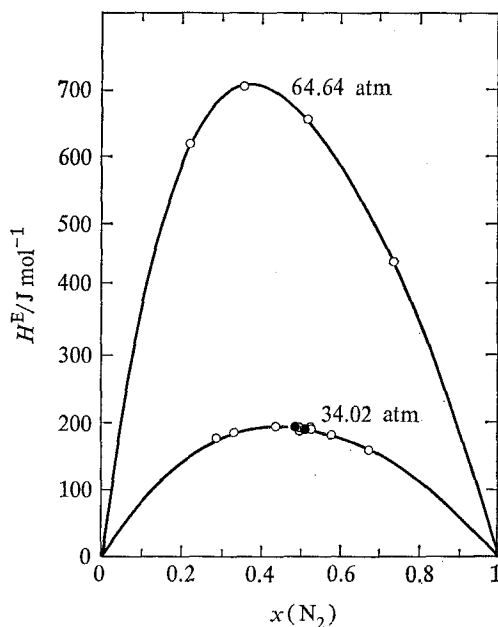


FIGURE 3. Excess enthalpy of N_2+O_2 at 40 °C. \circ , experimental value of H_n^E (the filled circles each represents three almost coincident points). The curve is the least squares fit.

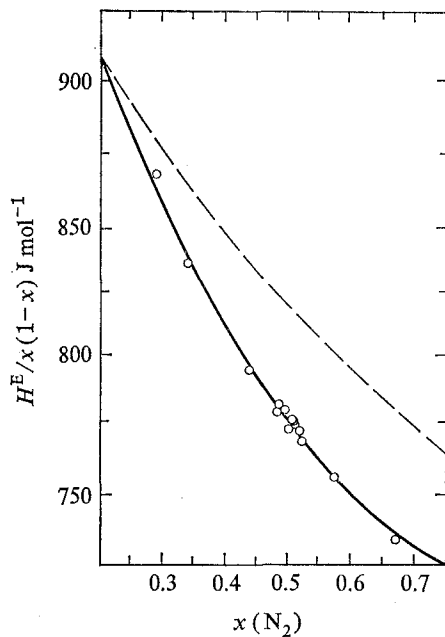


FIGURE 4. Excess enthalpy of the N_2+O_2 at $40^\circ C$ and 34.02 atm. Comparison with predictions by B.W.R. equation of state. The broken curve is that predicted by B.W.R. The unbroken curve is that obtained by the least squares fit. \circ , experimental value of H_n^E .

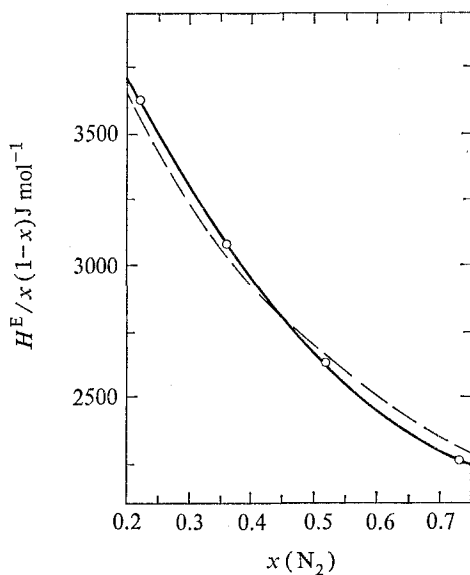


FIGURE 5. Excess enthalpy of N_2+CO_2 at $40^\circ C$ and 64.64 atm. Comparison with predictions by B.W.R. equation of state. The broken curve is that predicted by B.W.R. The unbroken curve is that obtained by the least squares fit. \circ , experimental value of H_n^E .

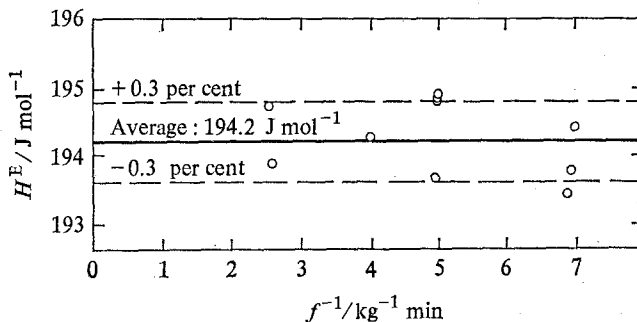


FIGURE 6. Excess enthalpy measurements of N_2+O_2 at 34.02 atm, 40 °C, and mole fraction 0.50 of nitrogen as a function of the specific flow rate f of the mixture. \circ , experimental value of H_n^E .

average value by 0.31 per cent—which is the same as the experimental precision. Hence a horizontal line was drawn, as shown in figure 6, and the assumption made that the heat leak \dot{q} is smaller than the experimental uncertainty.

ACCURACY

There are two factors that affect the accuracy of the experimental results. They are (1) inaccuracies in the instruments and experimental techniques and (2) errors introduced in the analysis of the results. The uncertainties introduced by the various factors are compounded using a procedure⁽²²⁾ which involves adding weighted individual accuracies. The weighting factors are obtained from a functional relation between the independent variables e.g. potentiometer accuracy, standard resistor accuracies. This method of error analysis yields an estimate of the maximum inaccuracy of the results. The estimated uncertainty in the measurement of temperature is 0.04 °C and of pressure is 0.02 atm at the calorimeter outlet. The uncertainty in the mole fraction is believed to be 0.002 to 0.003. The limit of accuracy of the primary corrections is believed to be 1.1 to 0.3 per cent based on the combined accuracy of the temperature and pressure difference measurements and of the heat capacity and isothermal Joule–Thomson coefficient. Based on the uncertainty in the calorimeter outlet pressure and temperature and in the excess heat capacity and excess isothermal Joule–Thomson coefficient, the maximum accuracy of the secondary corrections is estimated to be 0.1 to 0.3 per cent for the results at 34.02 atm and 0.3 to 1 per cent for the results at 64.64 atm. Adding the estimated accuracy of the electrical power input to the estimated accuracies of the primary and secondary corrections yields an accuracy of 0.8 to 1 per cent for the excess enthalpies at calorimeter outlet conditions, H_0^E , and 0.9 to 2 per cent for the normalized excess enthalpies, H_n^E .

COMPARISON WITH PREVIOUS WORK

The only data on N_2+CO_2 mixtures available to the authors were the published results of Lee and Mather.⁽⁶⁾ Their experimental conditions overlap with those of the present work at 40 °C and extend to higher pressures. The excess enthalpy values at 40 °C, both at 34.02 and 64.64 atm, agreed within the combined experimental error of both investigations.

COMPARISON WITH BENEDICT, WEBB, AND RUBIN EQUATION

Excess enthalpies were calculated with the original B. W. R. equation of state⁽¹⁷⁾ using the mixing rules of Benedict *et al.*⁽²⁰⁾ Various sets of constants were used: N₂: Crain and Sonntag,⁽²³⁾ Stotler and Benedict,⁽²⁴⁾ and Bloomer and Rao;⁽¹⁸⁾ CO₂: Eakin and Ellington,⁽²⁵⁾ and Cullen and Kobe.⁽¹⁹⁾ Various combinations of the constants for N₂ and CO₂ predicted approximately similar values of the excess enthalpy. However, the constants of Bloomer and Rao⁽¹⁸⁾ for N₂, and Cullen and Kobe⁽¹⁹⁾ for CO₂, give values of H^E that are closest to the experimental results reported here, and the broken lines in figures 4 and 5 represent calculations using these constants. The deviations from experimental results at 31 °C (43.02 and 64.64 atm) are similar to those at 40 °C at the same pressures.

The National Science Foundation provided support through two grants, NSF-GP-946 and NSF-GK-674. Dr Millard Jones designed the calorimeter mixing capsule and Dr David T. Mage contributed in the initial design and construction of the facility.

REFERENCES

1. Beenakker, J. J. M.; Coremans, J. M. J. *Second Symposium on Thermophysical Properties*. ASME: New York. 1962, p. 3.
2. Beenakker, J. J. M.; Van Eijnsbergen, B.; Knoester, M.; Taconis, K. W.; Zandbergen, P. *Third Symposium on Thermophysical Properties*. ASME: New York. 1965, p. 114.
3. Knoester, M.; Taconis, K. W.; Beenakker, J. J. M. *Physica (Utrecht)* 1967, 33, 389.
4. Van Eijnsbergen, B.; Beenakker, J. J. M. *Physica (Utrecht)* 1968, 39, 499.
5. Klein, R. R. Ph.D. Thesis, Yale University. 1969.
6. Lee, J. I.; Mather, A. E. *J. Chem. Thermodynamics* 1970, 2, 881.
7. Jacobsen, J. A.; Barieau, R. E. Paper presented at the 159th National Meeting of The American Chemical Society, Houston, Texas, February 22-27, 1970.
8. Cross, J. L. *Nat. Bur. Stand. (U.S.) Monogr.* 65, 1964.
9. Hejmadi, A. V. Forthcoming publication.
10. Bird, R. B.; Stewart, W. E.; Lightfoot, E. N. *Transport Phenomena*. John Wiley: New York. 1963.
11. Din, F. In *Thermodynamic Functions of Gases*, Vol. 3. F. Din, editor. Butterworths: London. 1961.
12. Newitt, D. M.; Pai, M. U.; Kuloor, N. R.; Huggill, J. A. W. In *Thermodynamic Functions of Gases*, Vol. 1. F. Din; editor. Butterworths: London. 1962.
13. Haney, R. E. D., Bliss, H. *Ind. Eng. Chem.* 1944, 36, 985.
14. Vukalovich, M. P.; Altunin, V. V. *Thermophysical Properties of Carbon Dioxide*. Collet's: London 1968.
15. Roebuck, J. R.; Murrell, T. A.; Miller, E. E. *J. Amer. Chem. Soc.* 1942, 64, 400.
16. Roebuck, J. R.; Osterberg, H. *Phys. Rev.* 1935, 48, 450.
17. Benedict, M.; Webb, G. B.; Rubin, L. C. *J. Chem. Phys.* 1940, 8, 334.
18. Bloomer, O. T.; Rao, K. N. *Inst. Gas Technol. Res. Bull.* 18, 1952.
19. Cullen, E. J.; Kobe, K. A. *AIChE J.* 1955, 1, 452.
20. Benedict, M.; Webb, G. B.; Rubin, L. C. *J. Chem. Phys.* 1942, 10, 747.
21. Montgomery, J. B.; De Vries, J. *J. Amer. Chem. Soc.* 1942, 64, 2372.
22. Mickley, H. S.; Sherwood, T. K.; Reed, C. E. *Applied Mathematics in Chemical Engineering*, McGraw-Hill: New York. 1957, p. 53.
23. Crain, R. W.; Sonntag, R. E. *J. Chem. Eng. Data* 1967, 12, 73.
24. Stotler, H. H.; Benedict, M. *Chem. Eng. Prog. Symp. Ser.* 6. 1953, 49, 25.